Frontiers of Information Technology & Electronic Engineering
www.zju.edu.cn/jzus; engineering.cae.cn; www.springerlink.com
ISSN 2095-9184 (print); ISSN 2095-9230 (online)
E-mail: jzus@zju.edu.cn

Real-time road traffic state prediction based on ARIMA and Kalman filter*

Dong-wei XU†[1,2], Yong-dong WANG[1,2], Li-min JIA[3], Yong QIN[3], Hong-hui DONG[3]

([1]*College of Information Engineering, Zhejiang University of Technology, Hangzhou 310023, China*)

([2]*United Key Laboratory of Embedded System of Zhejiang Province, Hangzhou 310023, China*)

([3]*State Key Laboratory of Rail Traffic Control and Safety, Beijing Jiaotong University 100044, China*)

†E-mail: dongweixu@zjut.edu.cn

Received Nov. 3, 2015; Revision accepted Feb. 26, 2016; Crosschecked Dec. 23, 2016

Abstract: The realization of road traffic prediction not only provides real-time and effective information for travelers, but also helps them select the optimal route to reduce travel time. Road traffic prediction offers traffic guidance for travelers and relieves traffic jams. In this paper, a real-time road traffic state prediction based on autoregressive integrated moving average (ARIMA) and the Kalman filter is proposed. First, an ARIMA model of road traffic data in a time series is built on the basis of historical road traffic data. Second, this ARIMA model is combined with the Kalman filter to construct a road traffic state prediction algorithm, which can acquire the state, measurement, and updating equations of the Kalman filter. Third, the optimal parameters of the algorithm are discussed on the basis of historical road traffic data. Finally, four road segments in Beijing are adopted for case studies. Experimental results show that the real-time road traffic state prediction based on ARIMA and the Kalman filter is feasible and can achieve high accuracy.

Key words: Autoregressive integrated moving average (ARIMA) model; Kalman filter; Road traffic state; Real-time; Prediction
http://dx.doi.org/10.1631/FITEE.1500381 **CLC number:** TP393; U491.13

1 Introduction

Considering the complex road conditions and traffic problems, road traffic state prediction has received increasing interest from researchers who have been investigating this topic in the past decade. Road traffic state prediction is not only an important foundation for traffic management and control, but also the key to formulate road traffic system guidance and a safe traffic strategy. Road traffic state prediction plays an important role in intelligent transportation systems. Besides, it is very useful in relieving traffic jams and making full use of road resources to predict the state of road traffic at future time intervals.

Many methods for predicting the state of road traffic have been proposed. Hoong *et al*. (2012) proposed a predictive analytic framework based on a Bayesian network for road condition prediction. Chang *et al*. (2011) established an advanced traffic management system that depends on obtaining complete data for dynamic traffic prediction. Recently, spatial-temporal correlations have stirred up the interest in road traffic prediction. Min and Wynter (2011) predicted the speed and volume of traffic at an interval of 5 min for up to 1 h in advance, based on a multivariate spatial-temporal autoregressive model, which proved to be fast and scalable for a full urban network. Pan *et al*. (2013) presented a stochastic cell transmission model framework to consider the spatial-temporal correlation of traffic flow and to conduct short-term traffic state prediction. Ma T *et al*. (2015) proposed a time-threshold vector error correction model for short-term traffic state prediction. Although

* Project supported by the National Science & Technology Pillar Program (No. 2014BAG01B02)
ORCID: Dong-wei XU, http://orcid.org/0000-0003-2693-922X

road traffic state prediction based on spatial-temporal correlations can achieve high accuracy, the traffic state of a specific site is greatly affected by its upstream and downstream traffic conditions, which are computationally intensive in different locations. Hidden Markov models also perform well in predicting short-term traffic conditions (Qi and Ishak, 2014). However, their changes in capacity can lead to unexpected outcomes. The *k*-nearest neighbor (*k*-NN) models also perform well in terms of short-term urban expressway flow prediction systems. Zhang *et al*. (2013) proposed an improved *k*-NN model for short-term traffic flow prediction. The algorithm is based on three components: an historical database, a search mechanism and algorithm parameters, and a prediction plan. The experiment was based on a section of Shanghai urban expressway. The accuracy of the algorithm can reach over 90%, and prove the feasibility of prediction of short-term road traffic states. A *k*-NN model combined with a wavelet neural network has also received attention. Lin *et al*. (2013) proposed an online short-term road traffic prediction based on a *k*-NN based local linear wavelet neural network. Results from the proposed method are better in terms of accuracy and running time than those of the *k*-NN based local linear wavelet neural network and support vector regression. Neural networks (NNs) and artificial neural networks (ANNs) have been applied in road traffic prediction in the past decade. NN traffic models trained with historical traffic data are capable of predicting the vehicle speed profile with current traffic information (Ma XL *et al*., 2015; Moretti *et al*., 2015; Park *et al*., 2011; Vlahogianni *et al*., 2005). Vlahogianni *et al*. (2005) proposed an optimized and meta-optimized NN for short-term traffic flow prediction. Park *et al*. (2011) and Ma XL *et al*. (2015) presented a short-term NN for traffic speed prediction. However, when developing NNs, researchers have to rely on time-consuming and questionably efficient rules of thumb because of limited knowledge of the network's optimal structure given a specific dataset. Liu *et al*. (2011) proposed a short-term road traffic prediction model with multiple dimensions based on support vector machine (SVM). They used the Global Positioning System (GPS) data of Guiyang City, China as an example, and compared the proposed model with the ARIMA model to test the reasonability of the method. An ANN for short-term traffic flow prediction using the past traffic data has also been investigated (Kumar *et al*., 2013; Sommer *et al*., 2015). Kumar *et al*. (2013) presented an ANN algorithm to predict speed data, and the ANN was trained using the data produced by a microscopic road traffic simulator. The test experiment of the method was based on a fixed interval of 30-min measurement, and the state prediction was conducted for different horizontal periods (5, 15, and 30 min). The method proved to be feasible in traffic speed prediction. Despite the advantages of SVM and ANN models, approaches sensitive to the quality of training data cannot be neglected. A hybrid model integrates the advantages of all types of single technologies, and achieves greater accuracy in short-term traffic speed prediction (Smith *et al*., 2002; Liu JY *et al*., 2012; Wang and Shi, 2013). However, installing this model in every traveler's car is expensive and time consuming. Recent efforts to improve traffic flow by using advanced information feedback (such as prediction feedback) with a cellular automaton (CA) model in intelligent transportation systems should also be remembered. Dong *et al*. (2009; 2010) introduced a prediction feedback strategy. The model incorporates the effects of adaptability into cellular automaton models of traffic flow. Simulation results adopting this optimal information feedback strategy demonstrate high efficiency in controlling the spatial distribution of traffic patterns. Chen *et al*. (2012) presented a feedback strategy, called the vacancy length feedback strategy (VLFS). Simulation results suggest that VLFS outperforms others in terms of value, stability, average flux, balance of the vehicle number, and the convenience of its application in real traffic conditions.

Apart from the aforementioned road traffic predictions, the autoregressive moving average (ARMA) model is one of the most widely used regression analysis methods, which aims to determine the type of regression relationship between historical data and future data (Smith *et al*., 2002; Chen *et al*., 2011; Durbin and Koopman, 2012; Lv *et al*., 2015). The autoregressive integrated moving average (ARIMA) model has been extensively applied to road traffic prediction. Chen *et al*. (2011) proposed an ARIMA with a generalized autoregressive conditional heteroscedasticity (ARIMA–GARCH) model for traffic flow prediction. A plane-moving average algorithm

was presented to solve the urban road flow forecasting problem (Lv *et al*., 2015). Smith *et al*. (2002) compared a seasonal ARIMA model and a nearest neighbor technique in predicting a 15-min expressway traffic flow around London. They concluded that the seasonal ARIMA model performs better than the nearest neighbor technique. Durbin and Koopman (2012) proposed a process of time series modeling and analysis by a state space method, and used the characteristics of the ARIMA model. Their work is a very useful introduction for researchers. The Kalman filter has been widely applied in stationary and non-stationary data analysis because of its favorable performance. The model is also computationally efficient, as it requires only an extremely small storage capacity, and is suitable for real-time traffic volume prediction. Zhang *et al*. (2012), Ojeda *et al*. (2013), and Guo *et al*. (2014) presented an adaptive Kalman filter for traffic flow prediction. Liu JY *et al*. (2012) proposed a hybrid model based on a Kalman filter and NN to predict the travel time from the Wenhui Bridge to the Mingguang Bridge in Shanghai, China. Data were collected by a mobile phone that supports GPS, and thus the feasibility of the hybrid model was validated. The Kalman filter can dynamically modify the prediction weight, and has high prediction accuracy. However, since road traffic time series is influenced by many factors and cannot be quantitatively analyzed, the estimation and measurement equations are difficult to obtain. Liu H *et al*. (2012) compared ARIMA–ANN and ARIMA–Kalman models in terms of wind speed prediction, and proved the superiority of the latter.

The models in most of these studies, especially spatial-temporal correlations and hidden Markov models, are excessively intensive in different locations and conditions. This study aims to develop a traffic prediction algorithm that is adequately robust and accurate to handle full-day road traffic state data. ANN, NN, and SVM have high accuracy in road traffic prediction, but their accuracy depends on the road traffic dataset and training quality. Hybrid models incorporate the advantages of single models, and thus they are extremely expensive and complex for travelers. Although the ARIMA model conducts short-term traffic prediction effectively, high prediction accuracy in a low-order ARIMA model and parameter estimation in a high-order ARIMA model are difficult to achieve.

Therefore, a real-time road traffic state prediction based on ARIMA and the Kalman filter (ARIMA–Kalman) is proposed in this study to solve the difficulties found in single modeling methods and to improve prediction accuracy. The contributions of the proposed algorithm are three fold:

1. A novel road traffic prediction algorithm, ARIMA–Kalman, is proposed to construct the measurement, state, and updating equations of the Kalman filter for road traffic prediction.

2. The proposed algorithm can determine optimal parameters through a training process based on the historical road traffic data.

3. A comparative study is conducted with four other algorithms to prove the feasibility of the proposed one.

2 Road traffic state prediction algorithm based on ARIMA and the Kalman filter

2.1 Framework

The main idea of the proposed road traffic state prediction algorithm is illustrated in Fig. 1. The historical traffic data are obtained from Beijing, China. The proposed algorithm constructs the ARIMA model based on historical road traffic data. The ARIMA model is then introduced into the Kalman filter to construct the state, measurement, and updating equations to complete the training process, using historical road traffic data. The optimal model parameters corresponding to the smallest absolute percentage error of the historical prediction results are determined

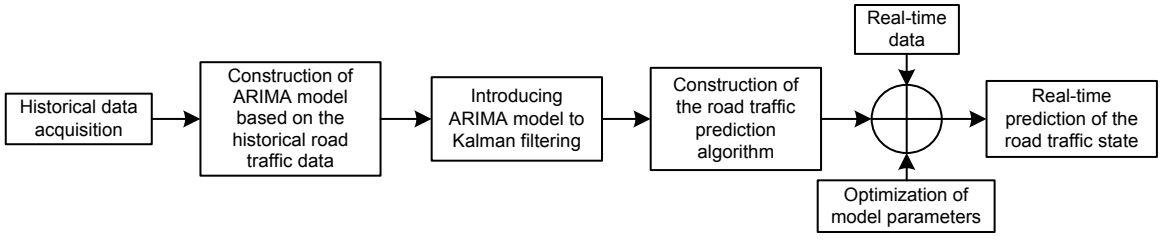

Fig. 1 Road traffic state prediction algorithm based on autoregressive integrated moving average and the Kalman filter

in the process. Finally, real-time road traffic data are introduced into the proposed algorithm to complete the real-time road traffic data prediction.

2.2 Modeling the road traffic ARIMA model of a time series

When modeling an ARIMA model in a time series, the series should be stationary. A non-stationary time series can become stationary when a differencing technique is used to handle it. If the time series x_t to be studied is non-stationary, a stationary series can be obtained in a standard ARIMA model by proper differencing (Brockwell and Davis, 2006; Kirchgässner *et al*., 2012):

$$\begin{cases} \varphi(B)(1-B)^d x_t = \theta(B)a_t, \\ \varphi(B) = 1-\varphi_1(t)B-\varphi_2(t)B^2-\cdots-\varphi_p(t)B^p, \\ \theta(B) = 1-\theta_1(t)B-\theta_2(t)B^2-\cdots-\theta_q(t)B^q, \end{cases} \quad (1)$$

where t=1, 2, … is the serial number, $\{x_t\}$ is the time series, $\{\alpha_t\}$ is the normal white noise process, with a mean value of zero and a variance of σ^2, $\varphi_i(t)$ (i=1, 2, …, p) and $\theta_j(t)$ (j=1, 2, …, q) are the parameters that must be estimated, p is the order of autoregressive (AR) polynomial, q is the order of moving average (MA) polynomial, B is the backshift operator, d is the order of differencing, $\varphi(B)$ is the AR polynomial, and $\theta(B)$ is the MA polynomial.

The stationary time series can be used to formulate an ARIMA model and determine its order and parameters. The order (p, q) can be preliminarily determined using the autocorrelation function (ACF) feature and the partial ACF (PACF) feature of the stationary time series. Finally, (p, q) can be determined using the Akaike information criterion (AIC). The stationary nature and reversibility of the estimated parameters can be validated by solving the equations of the ARIMA model to determine the model parameters. In the analysis of time series, the Yule–Walker equation plays an important role in pattern recognition and parameter estimation. Thus, the Yule–Walker equation is introduced in this study. The residual of the ARIMA model can be regarded as the model estimation criterion. A likelihood maximization method is used in the model estimation procedure. By solving the ACF of the residual, we can judge whether the residual series is white noise or not. If the residual series is not white noise, (p, q) will be redefined.

Therefore, the road traffic state at moment t+1 can be predicted and described as follows:

$$\begin{aligned} x(t+1) = {} & \varphi_1(t)x(t)+\varphi_2(t)x(t-1)+\cdots \\ & +\varphi_p(t)x(t-p+1)+e(t+1) \\ & -\theta_1(t)e(t)-\theta_2(t)e(t)-\cdots \\ & -\theta_q(t)e(t-q+1), \end{aligned} \quad (2)$$

where $\{x(t+1), x(t), \ldots, x(t-p+1)\}$ is the road traffic series corresponding to moments $\{t+1, t, \ldots, t-p+1\}$, $\varphi_1(t)$, $\varphi_2(t)$, …, $\varphi_p(t)$ are the autoregressive coefficients at moment t, $\{\theta_1(t), \theta_2(t), \ldots, \theta_q(t)\}$ is the moving average coefficients series at moment t, and $\{e(t+1), e(t), \ldots, e(t-q+1)\}$ is the noise series, which is normally distributed, corresponding to moment $\{t+1, t, \ldots, t-p+1\}$.

Seasonal ARIMA (SARIMA) models reflect the feature of seasonal variation in time series, and can be divided into simple and multiple models. The seasonal component will be considered in this study. Generally, the original time series $\{X_t\}$ uses a lag operator B to process SARIMA (p, d, q)(P, D, Q). A seasonal ARIMA model can be written as

$$\begin{cases} \phi_p(B)(B^S)^d(1-B^S)^D X_t = \theta_q(B)\Theta_Q(B^S)\varepsilon_t, \\ \Phi_p(B^S) = 1-\Phi_S B^S-\Phi_{2S}B^{2S}-\cdots-\Phi_{PS}B^{PS}, \\ \Theta_Q(B^S) = 1-\Theta_S B^S-\Theta_{2S}B^{2S}-\cdots-\Theta_{QS}B^{QS}, \end{cases} \quad (3)$$

where $\Phi_P(B^S)$ and $\Theta_Q(B^S)$ are polynomial in B of degrees P and Q, respectively, P is the order of seasonal autoregression, D is the number of seasonal differences, Q is the order of the seasonal moving average, and S is the length of the season.

2.3 Construction

The Kalman filter solves the best linear filter problem based on the criterion of minimum mean square error. The best estimation of the state variables for the filter is made by a recursive algorithm. By computing the state and measurement equations, the former estimation, and the latest observations, we can estimate the current value to acquire the best estimation data. The Kalman filter method has many advantages. It relies only on the recursive method and

does not require all the historical data. It can be used to deal with not only the stationary and non-stationary random processes, but also time-varying and non-time-varying systems. Generally, the observation and measurement equations of the Kalman filter are described in Eqs. (4) and (5), respectively:

$$\boldsymbol{X}_{t+1}=\boldsymbol{A}\boldsymbol{X}_t+\boldsymbol{W}_t, \tag{4}$$

$$\boldsymbol{Y}_t=\boldsymbol{B}\boldsymbol{X}_t+\boldsymbol{V}_t, \tag{5}$$

where $\boldsymbol{X}_{t+1}$ and $\boldsymbol{Y}_t$ are n-dimensional state vector and m-dimensional observation vector of the system, respectively, $\boldsymbol{A}$ and $\boldsymbol{B}$ are $m\times n$-dimensional state transition matrix and observation matrix, respectively, and $\boldsymbol{W}_t$ and $\boldsymbol{V}_t$ are n-dimensional random interference vector and m-dimensional observed noise vector of the system, respectively.

Determining the state and observation equations is difficult, because the single road traffic state time series cannot effectively reflect the road traffic state. Thus, the mathematical expression of the ARIMA model is introduced into the state and measurement equations of the Kalman filter to predict the road traffic state.

If $x_1(t)=x(t)$, $x_2(t)=x(t-1)$, …, $x_p(t)=x(t-p+1)$, $e_1(t)=e(t)$, $e_2(t)=e_1(t-1)$, …, $e_q(t)=e_{q-1}(t-1)$, the ARIMA model of road traffic data is introduced into the state and measurement equations of the Kalman filter prediction algorithm. The ARIMA model can be described as follows:

$$\begin{aligned} x_1(t+1)=&\varphi_1(t)x_1(t)+\varphi_2(t)x_2(t)+\cdots+\varphi_p(t)x_p(t)\\ &+e_1(t+1)-\theta_1(t)e_1(t)-\theta_2(t)e_2(t)-\cdots\\ &-\theta_q(t)e_q(t), \end{aligned} \tag{6}$$

where $\{x_1(t), x_2(t), \ldots, x_p(t)\}$ corresponds to the road traffic data sequence $\{1, 2, \ldots, p\}$ at moment t.

From Eq. (6), we can find $x_2(t+1)=x_1(t)$, $x_3(t+1)=x_2(t)$, …, $x_{p+1}(t+1)=x_p(t)$, $e_2(t+1)=e_1(t)$, $e_3(t+1)=e_2(t)$, …, $e_q(t+1)=e_{q-1}(t)$. Eq. (6) can be described as

$$\begin{aligned} \begin{bmatrix} x_1(t+1)\\ x_2(t+1)\\ \vdots\\ x_p(t+1) \end{bmatrix} &= \begin{bmatrix} \varphi_1(t) & \varphi_2(t) & \cdots & \varphi_p(t)\\ 0 & 1 & \cdots & 0\\ \vdots & \vdots & & \vdots\\ 0 & 0 & \cdots & 1 \end{bmatrix} \begin{bmatrix} x_1t\\ x_2t\\ \vdots\\ x_pt \end{bmatrix}\\ &+\begin{bmatrix} 1\\ 0\\ \vdots\\ 0 \end{bmatrix} e_1(t+1)+\begin{bmatrix} -\theta_1(t)\\ 0\\ \vdots\\ 0 \end{bmatrix} e_1(t)+\ldots+\begin{bmatrix} -\theta_q(t)\\ 0\\ \vdots\\ 0 \end{bmatrix} e_q(t). \end{aligned} \tag{7}$$

From Eqs. (2), (4), (5), (6), and (7), the observation equation can be written as follows:

$$\begin{aligned} \boldsymbol{Y}(k+1)=&[1,0,\cdots,0][x_1(k+1),x_2(k+1),\cdots,\\ &x_p(k+1)]^{\mathrm{T}}. \end{aligned} \tag{8}$$

The ARIMA–Kalman prediction algorithm uses the state and observation equations to express the Kalman filter equations as Eqs. (7) and (8). Combined with the iterator, the Kalman filter can be updated. The specified equations can be described as follows:

$$\boldsymbol{P}(t+1|t)=\boldsymbol{A}\cdot\boldsymbol{P}(t|t)'+\boldsymbol{R}_1+\boldsymbol{R}_2+\ldots+\boldsymbol{R}_q, \tag{9}$$

$$\mathrm{Kg}(t+1)=\boldsymbol{P}(t+1|t)\cdot\boldsymbol{B}'/(\boldsymbol{B}\cdot\boldsymbol{P}(t+1|t)\cdot\boldsymbol{B}'+\boldsymbol{Q}), \tag{10}$$

$$\boldsymbol{X}(t+1|t+1)=\boldsymbol{X}(t+1|t)+\mathrm{Kg}(t+1)\cdot(\boldsymbol{Z}(t+1)-\boldsymbol{B}\cdot\boldsymbol{X}(t|t)), \tag{11}$$

$$\boldsymbol{P}(t+1|t+1)=(\boldsymbol{I}-\mathrm{Kg}(t+1)\cdot\boldsymbol{B})\cdot\boldsymbol{P}(t+1|t), \tag{12}$$

where $\boldsymbol{X}(t+1|t)$ is the road traffic prediction value at moment $t+1$ based on that at moment t, $\boldsymbol{P}(t+1|t)$ is covariance matrix corresponding to $\boldsymbol{X}(t+1|t)$, $(R_1, R_2, \ldots, R_q)$ is the covariance matrix corresponding to $(e_1, e_2, \ldots, e_q)$, $\boldsymbol{Q}$ is the covariance matrix of the observation noise equation, $\boldsymbol{B}$ is the observation matrix, Kg is the error gain, and $\boldsymbol{Z}$ is the observed vector. Through the aforementioned equations, the prediction results can be described as

$$\boldsymbol{Y}(t+1)=\boldsymbol{B}\boldsymbol{X}(t+1|t+1), \tag{13}$$

where $\boldsymbol{Y}(t+1)$ is the road traffic value at moment $t+1$, and $\boldsymbol{X}(t+1|t+1)$ is the optimal estimation vector of the road traffic data at moment $t+1$.

2.4 Prediction of real-time road traffic state based on the proposed algorithm

Historical data are preprocessed to establish the ARIMA model. ACF and PACF are calculated to preliminarily determine the scope of the model structure parameters (p, q). Then, the best (p, q) values are determined using the AIC criterion. In the process of determining model construction, we conduct a Kwiatkowski–Phillips–Schmidt–Shin (KPSS) test on the initial time series. The value of p is 0.010. Thus, we could argue that the time series is not stationary. Then, one difference in the value of p of the time series of the augmented Dickey–Fuller (ADF) test is less than 0.001. Thus, we could determine that the value of d is 1.

According to the AIC criterion, we can find the optimal (p, q). The ARIMA model structure of the road traffic time series x_t is eventually identified as (1, 1, 1). The parameter estimation also varies because of the different amount of historical data used for modeling. Therefore, the model can be generally described as follows:

$$x(t)=\varphi_1(t)x(t-1)+\varphi_2(t)x(t-2)+e(t)-\theta_1(t)e(t-1). \quad (14)$$

Then, Eq. (14) can be described as follows:

$$\begin{aligned} x(t+1)=&\varphi_1(t+1)x(t)+\varphi_2(t+1)x(t-1)\\ &+e(t+1)-\theta_1(t+1)e(t). \end{aligned} \quad (15)$$

From the Kalman filter prediction algorithm formula and Eq. (6), Eq. (13) can be described as follows:

$$\begin{aligned} \begin{bmatrix} x_1(t+1) \\ x_2(t+1) \end{bmatrix} =& \begin{bmatrix} \varphi_1(t+1) & \varphi_2(t+1) \\ 0 & 1 \end{bmatrix} \begin{bmatrix} x_1(t) \\ x_2(t) \end{bmatrix} \\ &+ \begin{bmatrix} 1 \\ 0 \end{bmatrix} e_1(t+1) + \begin{bmatrix} -\theta_1(t) \\ 0 \end{bmatrix} e_1(t). \end{aligned} \quad (16)$$

The state variables in the experiments are the historical road traffic volume and speed at the current moment, and the observed measurements are the predicted volume and speed data at the next moment.

3 Parameter determination

The following parameters are used in the process of road traffic data prediction based on ARIMA–Kalman: The ARIMA model parameters are $\varphi_1(t)$, $\varphi_2(t)$, $\theta_1(t)$, which can be determined by the model construction parameters (p, d, q) and the number N of the historical data used for modeling. The Kalman filter parameters include the dimension state transition matrix $\boldsymbol{A}$, observation matrix $\boldsymbol{B}$, state noise vector $\boldsymbol{W}_t$, and observed noise vector $\boldsymbol{V}_k$, which are determined by the model construction (p, d, q). The initial state $\boldsymbol{X}(0)$ and covariance matrix $\boldsymbol{P}(0|0)$ can be determined by experience. With regard to the historical road traffic data at different moments, different road traffic data models corresponding to various road traffic state parameters (p, d, q, N) can be obtained. Parameter setting is concerned only with the analysis of the effect of the road traffic state prediction algorithm based on ARIMA–Kalman. Separately analyzing the effect of each parameter on the accuracy of the algorithm does not guarantee the optimal algorithm, because these parameters have different influences on the accuracy of the algorithm. All the parameters in the road traffic state prediction results should be considered when conducting the algorithm analysis.

The mean absolute relative error (marerr) of prediction data is introduced to measure the effects of parameters on the algorithm accuracy:

$$\text{marerr}=\frac{1}{N}\sum_t \frac{|x_{\text{pred}}(t)-x_{\text{real}}(t)|}{x_{\text{real}}(t)}, \quad (17)$$

where x_{pred} and x_{real} are the predicted and real road traffic states, respectively.

For different (p, d, q, N)'s, there are corresponding values of marerr, which means that there is a distribution relationship w between (p, d, q, N) and marerr. Thus, the following formula can be obtained:

$$\text{marerr}=w(p, d, q, N). \quad (18)$$

The process of finding the minimum marerr corresponding to (p, d, q, N) involves training optimal parameters. Thus, we obtain the following model:

$$\min \omega(p, d, q, N), \quad (19)$$

which is subject to Eq. (17).

Finally, the values of (p, d, q, N) can be determined by statistical analysis of road traffic state prediction results.

4 Experiments

4.1 Data acquisition

Four sets of road speed and volume data were adopted in this study (Table 1). To achieve a better performance, the road traffic state data under the same running mode were extracted for training and prediction. The road traffic speed and volume data captured on June 15, 16, 18, and 19, 2011 were extracted as historical road traffic state data to train optimal parameters. The road traffic speed and

volume data captured on June 22, 23, 25, and 26, 2011 were extracted to make a road traffic state prediction. June 15 and 22 were Wednesday, June 16 and 23 were Thursday, June 18 and 25 were Saturday, and June 19 and 26 were Sunday. Therefore, we used the training parameters based on the data of June 15, 16, 18, and 19, to predict in real time the road traffic speed and volume values of June 22, 23, 25, and 26, respectively. The traffic speed and volume data collection interval was 2 min.

Table 1 Road segment information

ID	Road segment
HI7000d	Xiaojie Bridge East to Dongzhimen Bridge
HI2075a	Central Conservatory of Music to Xibianmen Bridge
HI7008a	White Bridge to Guangqumen Road
HI3002b	Deshengmen Bridge to Jishuitan Bridge

The proposed algorithm was compared with a pure ARIMA model and a Kalman filter method to ensure an appropriate comparison. The pure ARIMA model and Kalman filter method employed in the study used the fixed and nearest-neighbor road traffic speed and volume data numbers (which is 15 here) to design the ARIMA model and Kalman filter method for real-time road traffic speed and volume prediction. The road traffic speed and volume data on June 22, 23, 25, and 26 were used for real-time prediction with the proposed method, the pure ARIMA model, and the Kalman filter method. The study was conducted for a 20-min interval prediction. The x-axis indicates time, and y-axis indicates the speed and volume values. The road traffic state data we used were limited. From the time series diagram, we found that the road traffic state did not show obvious seasonal characteristics. Thus, we took no account of seasonal components in the modeling.

Long memory fractionally differenced ARIMA (ARFIMA) models have been used in various fields. Thus, the ARFIMA process was considered in our study. We estimated the fractional difference, and then estimated p and q. The estimation method we used was the maximum likelihood method. Considering the road traffic state data, d was 4.583013×10^{-5}, which proved that the long memory is not obvious. We also chose an AIC of (1, 1, 1). All the AICs are described in Table 2.

From Table 2, we find that (1, 1, 1) is the optimal model construction. Thus, we used (1, 1, 1) as the best model construction.

Table 2 Statistical results of AIC

(p, d, q)	AIC
$(1, 4.583013\times10^{-5}, 1)$	5687.44
$(1, 4.583013\times10^{-5}, 2)$	5689.31
$(2, 4.583013\times10^{-5}, 1)$	5689.28
$(2, 4.583013\times10^{-5}, 2)$	5688.96
(1, 1, 1)	5675.85

AIC: Akaike information criterion

4.2 Results

The speed prediction results for the four road segments are illustrated in Figs. 2–5, in each of which the results for June 22, 23, 25, and 26 are presented as (a), (b), (c), and (d), respectively. The volume prediction results for the four road segments are shown in Figs. 6–9, in each of which the results for June 22, 23, 25, and 26 are presented as (a), (b), (c), and (d), respectively.

To present a clear comparison, the statistical results from particle filtering and the expectation-maximization are included. The statistical results of the predicted speed and volume on June 22, 23, 25, and 26, 2011 are listed in Tables 3–14. marerr, mxarer, and rmrerr represent the mean absolute relative error, the maximum absolute relative error, and the mean relative error sum of squares, respectively. The average is the mean value of the three indicators of the four segments. marerr is described in Eq. (17). mxarer and rmrerr can be described as follows:

$$\text{mxarer} = \max\left|\frac{x_{\text{pred}}(t)-x_{\text{real}}(t)}{x_{\text{real}}(t)}\right|, \tag{20}$$

$$\text{rmrerr} = \frac{1}{N}\left(\frac{x_{\text{pred}}(t)-x_{\text{real}}(t)}{x_{\text{real}}(t)}\right)^2. \tag{21}$$

Let ma_{AK}, ma_{A}, ma_{KF}, ma_{PF}, and ma_{EM} denote the marerr of ARIMA–Kalman, ARIMA model, Kalman filter, particle filter, and expectation maximization, respectively. Let mx_{AK}, mx_{A}, mx_{KF}, mx_{PF}, and mx_{EM} denote the mxarer of ARIMA–Kalman, ARIMA model, Kalman filter, particle filter, and expectation maximization, respectively. Let rm_{AK}, rm_{A}, rm_{KF}, rm_{PF}, and rm_{EM} denote the rmrerr

of ARIMA–Kalman, ARIMA model, Kalman filter, particle filter, and expectation maximization, respectively.

4.3 Statistical test

Given the same theoretical background of ARIMA–Kalman and ARIMA models, the statistical significance of the measurements could be assessed. We used a statistical test proposed by Diebold and Mariano (1995). Based on their suggestion, the asymptotic test (S_1) was used in this study, described as follows:

$$S_1 = \overline{d} \Big/ \sqrt{2\pi \overline{f_d(0)} / n}. \tag{22}$$

$\{d_i\}$ is the loss-differential series of ARIMA–Kalman and ARIMA models, defined as

$$d_i = e_{\mathrm{AK}}^2 - e_{\mathrm{A}}^2,\ i \in \mathbb{R}. \tag{23}$$

The weighted sum of the available sample autocovariances is

$$2\pi \overline{f_d(0)} = \frac{1}{n} \sum_{i=1}^{n} (d_i - \overline{d})^2, \tag{24}$$

where n is the sample size.

If the absolute value of S_1 is smaller than 1, the two models would have the same ability of measurement. If the value of S_1 is greater than 1, the loss–differential function of the ARIMA–Kalman model would be markedly greater than that of the ARIMA model. This result would indicate that the ARIMA model is better able to measure the road traffic. If the value of S_1 is smaller than −1, the loss–differential function of the ARIMA–Kalman model would be significantly smaller than that of the ARIMA model. This result would imply that the ARIMA–Kalman model is better able to measure road traffic.

The experimental results on different links were used for the statistical test. The statistical significance results are shown in Table 15, from which we can see that the ARIMA–Kalman model is generally better able to predict speed and volume.

4.4 Analysis of experimental results

From Figs. 2–9 and Tables 3–14, we see that:

1. The road traffic state (speed and volume) predictions based on the ARIMA–Kalman model are superior to those according to other four algorithms.

From Figs. 2–9, the accuracy and stability of speed and volume predicted based on the ARIMA–Kalman model are superior to those based on the other four algorithms for all the segments.

We find that for all experiment road segments, the accuracy and stability of speed and volume predicted based on the ARIMA–Kalman model are superior to those based on the pure ARIMA model, Kalman filter, and particle filter. The stability of speed and volume predicted based on the ARIMA–Kalman model is inferior to that from expectation maximization.

Tables 15 shows that the ARIMA–Kalman model is strikingly superior to the pure ARIMA model.

2. The accuracy of speed prediction is higher than that of volume prediction.

The regularity of the change in volume is determined mainly by the regularity of people's travel origin-destination (OD). However, for different dates, people's travel OD changes randomly. So, the regularity of change in volume has a certain random property. The regularity of change in speed is affected not only by the regularity of people's OD travel but also by the running status of road infrastructure. Thus, the change in speed shows high regularity. The accuracy of speed is consequently higher than that of volume when they are estimated on the basis of the regularity of road traffic.

3. There are still some errors in predicting road traffic states using this algorithm.

There are two main reasons for these errors: (1) Obtaining the corresponding road traffic states with a perfect match based on the ARIMA–Kalman model is difficult, because of the limitations of the road traffic running characteristics. (2) The parameters exhibit a certain deviation. Determining the optimal parameters is irregular, because they vary for different road traffic state data sets. The selected optimal parameters are determined based on historical road traffic state data. Therefore, the current optimal parameters may be different from the historical optimal parameters.

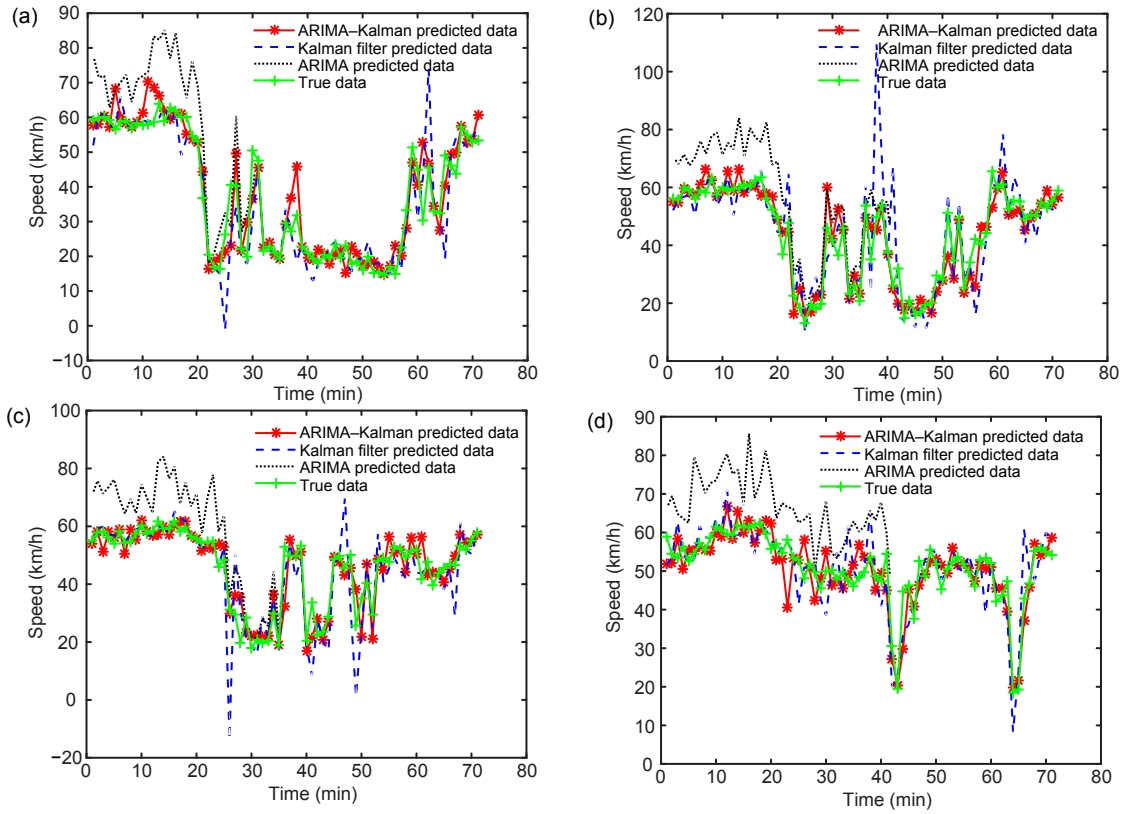

Fig. 2 Speed prediction results of HI2075a on June 22 (a), 23 (b), 25 (c), and 26 (d), 2011

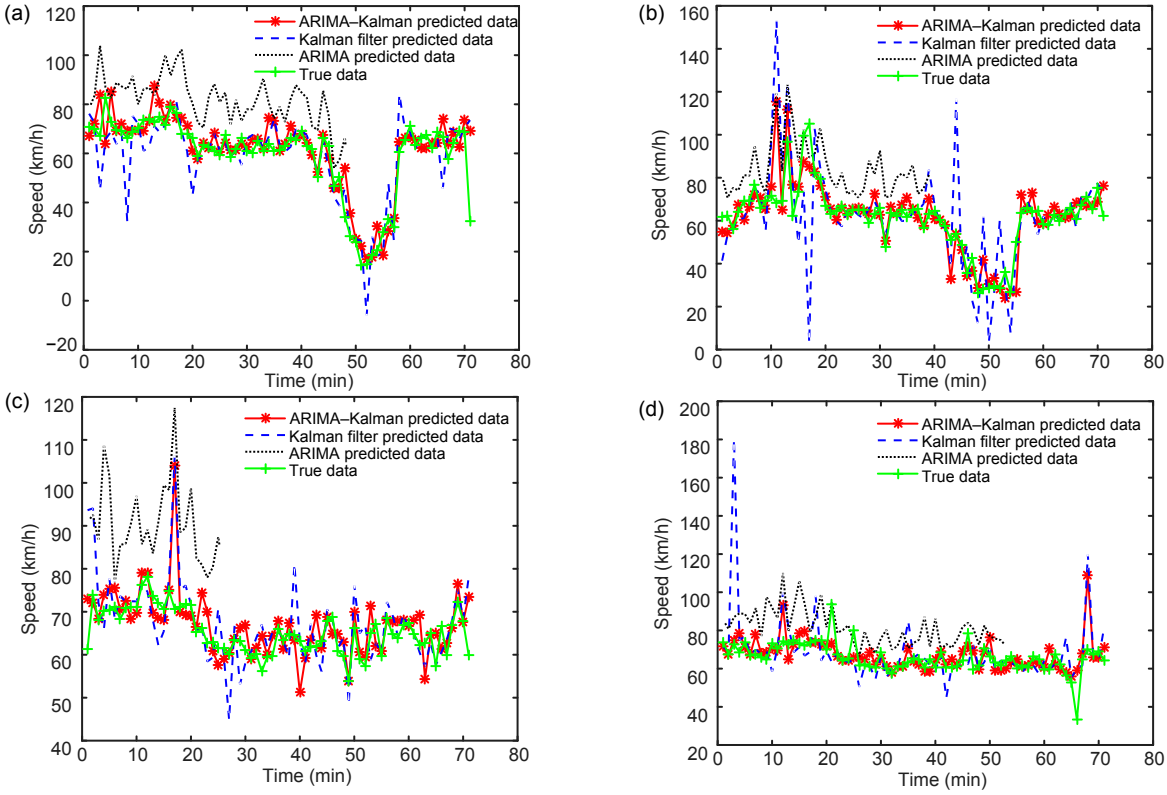

Fig. 3 Speed prediction results of HI3002b on June 22 (a), 23 (b), 25 (c), and 26 (d), 2011

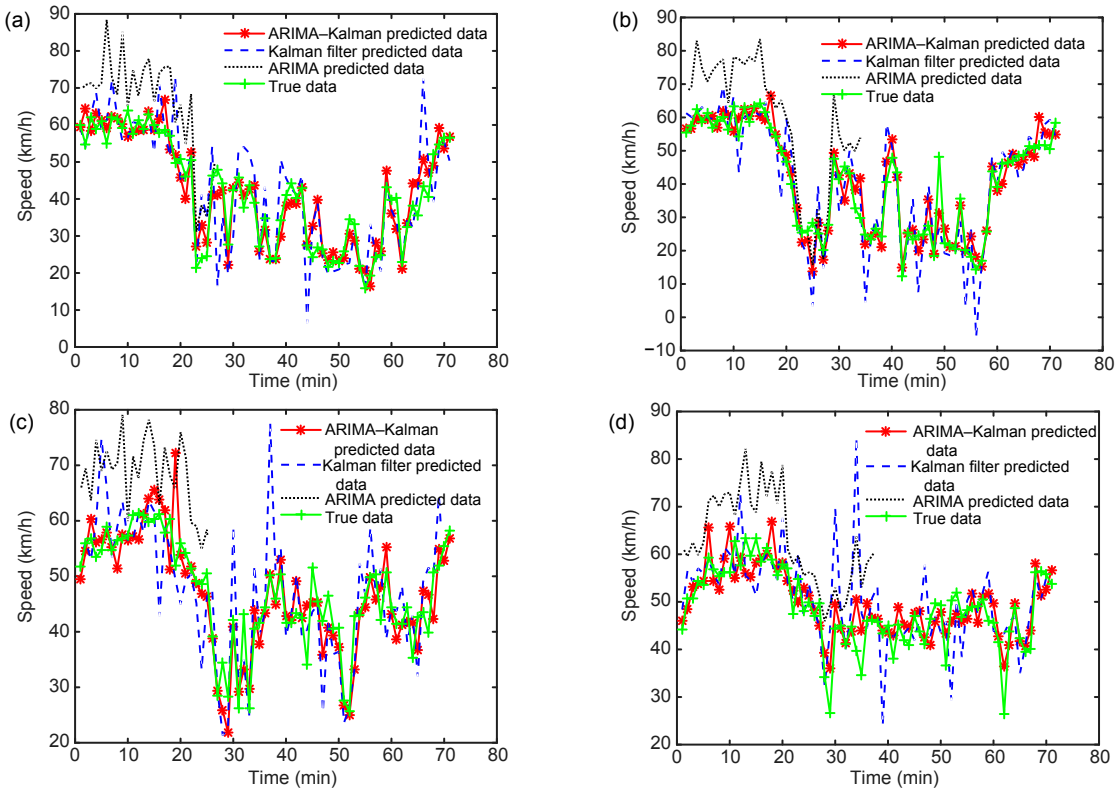

Fig. 4 Speed prediction results of HI7000d on June 22 (a), 23 (b), 25 (c), and 26 (d), 2011

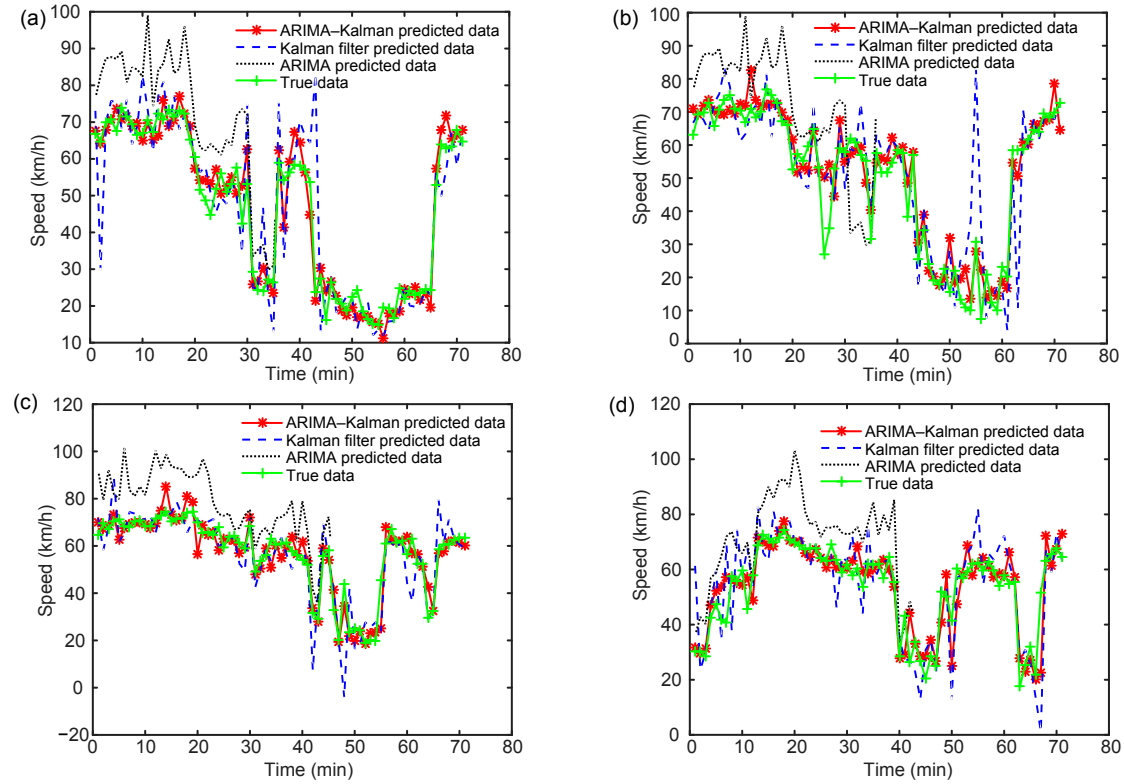

Fig. 5 Speed prediction results of HI7008a on June 22 (a), 23 (b), 25 (c), and 26 (d), 2011

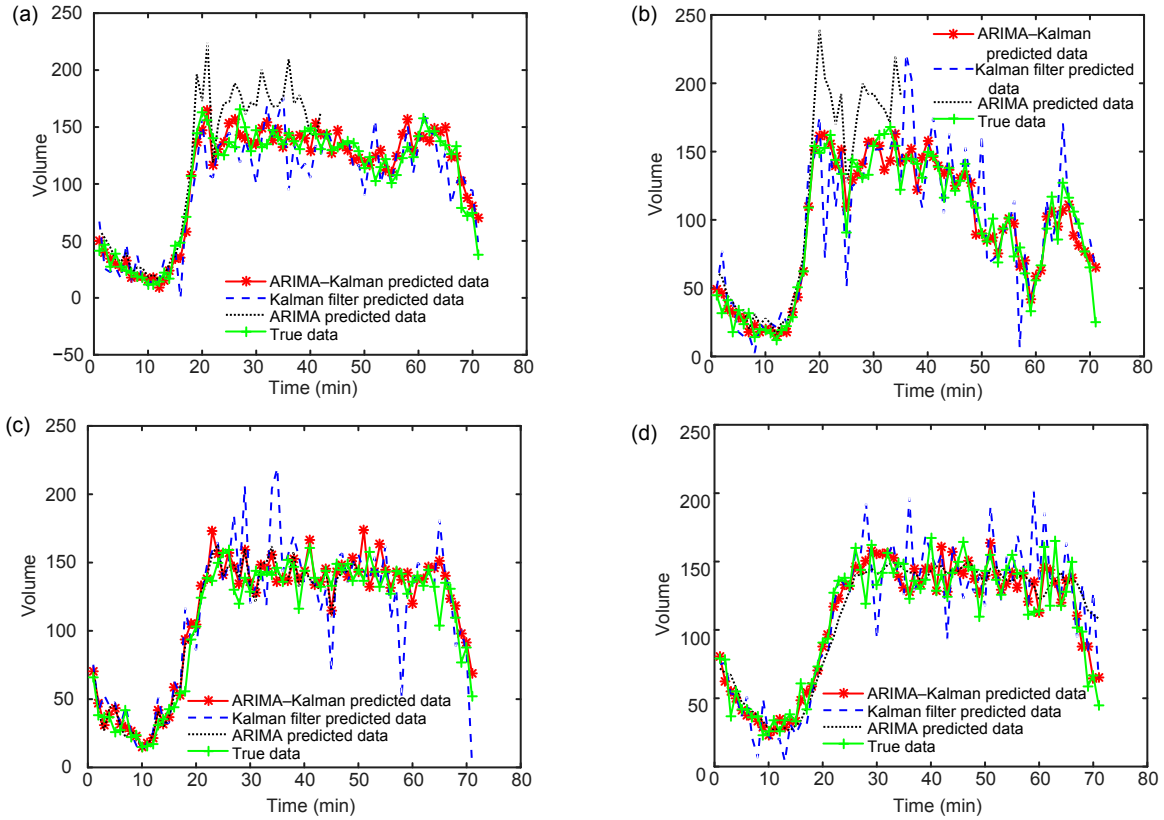

Fig. 6 Volume prediction results of HI2075a on June 22 (a), 23 (b), 25 (c), and 26 (d), 2011

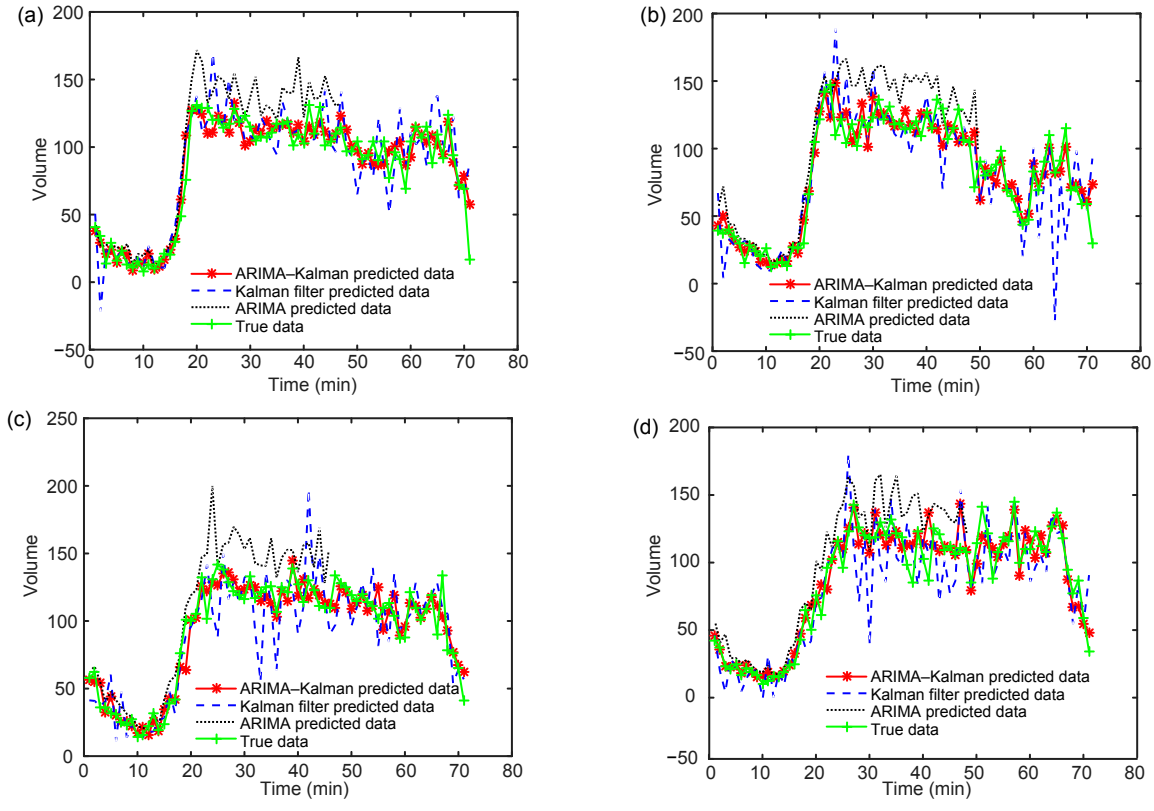

Fig. 7 Volume prediction results of HI3002b on June 22 (a), 23 (b), 25 (c), and 26 (d), 2011

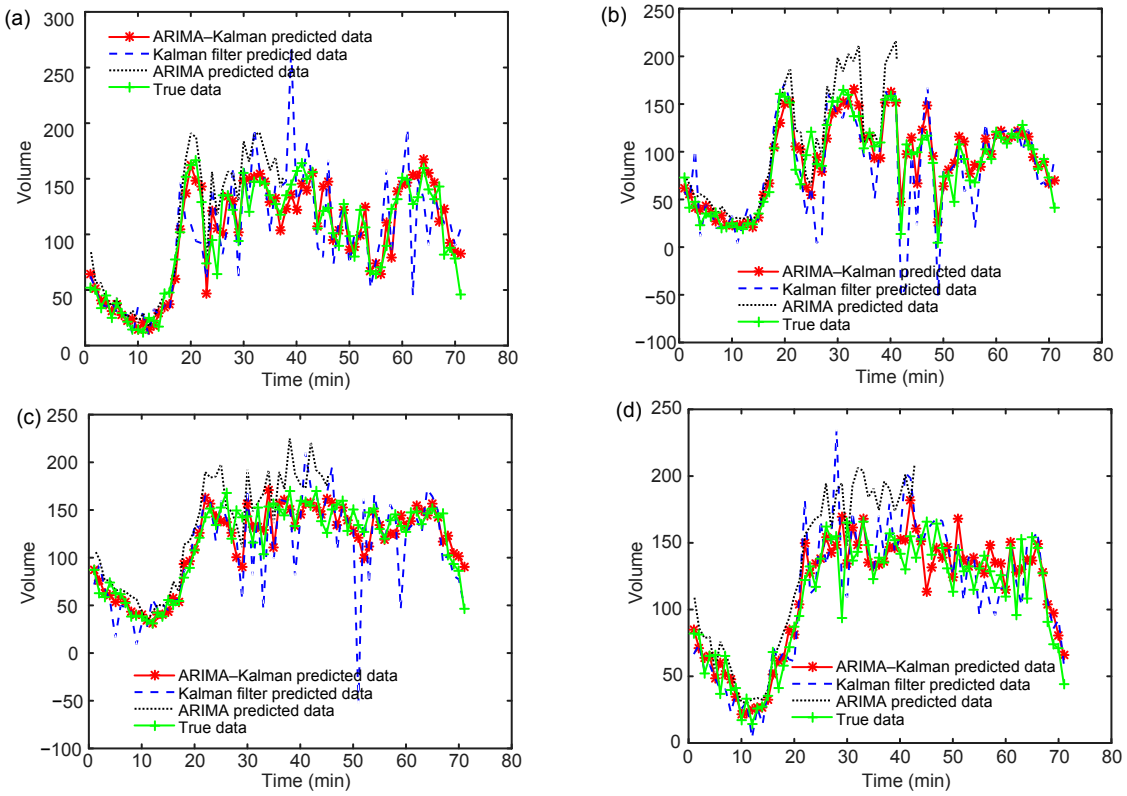

Fig. 8 Volume prediction results of HI7000d on June 22 (a), 23 (b), 25 (c), and 26 (d), 2011

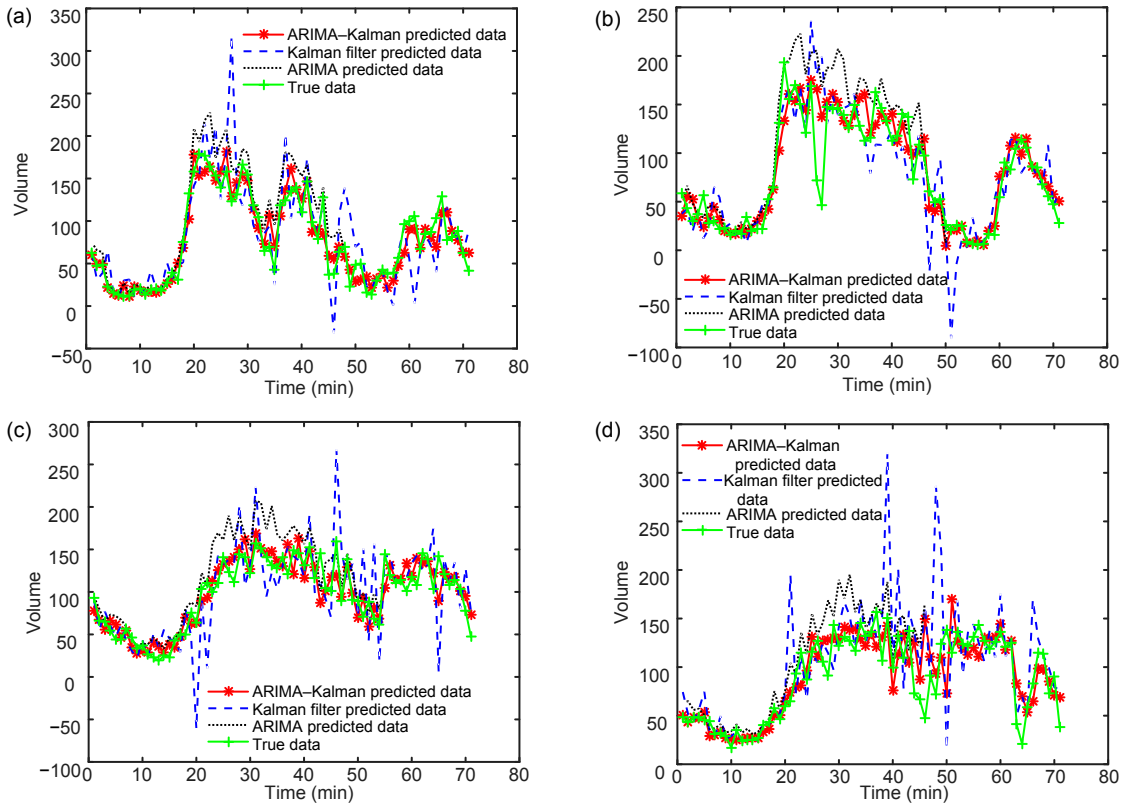

Fig. 9 Volume prediction results of HI7008a on June 22 (a), 23 (b), 25 (c), and 26 (d), 2011

Table 3 Mean absolute relative error of speed on June 22 and 23, 2011

Segment	Mean absolute relative error (%)									
	June 22, 2011					June 23, 2011				
	ma_{AK}	ma_{A}	ma_{KF}	ma_{PF}	ma_{EM}	ma_{AK}	ma_{A}	ma_{KF}	ma_{PF}	ma_{EM}
HI2075a	12.41	14.13	27.66	21.08	26.13	10.63	17.98	25.85	18.29	22.82
HI3002b	10.61	14.96	32.00	12.67	14.33	9.39	21.10	25.45	11.64	16.62
HI7000d	9.59	17.24	25.98	18.67	22.07	9.77	19.30	26.81	20.45	23.70
HI7008a	9.19	19.42	23.97	18.36	22.81	17.11	31.13	35.12	31.29	21.24
Average	10.45	16.44	27.40	17.70	21.34	11.73	22.38	28.31	20.42	21.10

Table 4 Mean absolute relative error of volume on June 22 and 23, 2011

Segment	Mean absolute relative error (%)									
	June 22, 2011					June 23, 2011				
	ma_{AK}	ma_{A}	ma_{KF}	ma_{PF}	ma_{EM}	ma_{AK}	ma_{A}	ma_{KF}	ma_{PF}	ma_{EM}
HI2075a	13.37	20.95	29.67	67.17	14.69	14.5	26.98	34.53	52.39	19.01
HI3002b	15.43	28.11	32.82	66.71	19.16	13.71	27.69	30.59	46.68	18.38
HI7000d	17.18	31.18	31.21	48.21	16.66	25.3	49.06	47.61	69.27	41.83
HI7008a	21.46	45.25	35.75	64.23	30.12	25.88	54.55	40.84	77.95	26.02
Average	16.86	31.37	32.36	61.58	20.16	19.85	39.57	38.39	61.57	26.31

Table 5 Maximum absolute relative error of speed on June 22 and 23, 2011

Segment	Maximum absolute relative error (%)									
	June 22, 2011					June 23, 2011				
	mx_{AK}	mx_{A}	mx_{KF}	mx_{PF}	mx_{EM}	mx_{AK}	mx_{A}	mx_{KF}	mx_{PF}	mx_{EM}
HI2075a	73.53	103.96	79.54	138.20	67.06	117.14	156.24	91.50	108.82	62.32
HI3002b	111.74	141.18	195.11	110.88	90.23	154.20	124.10	75.43	72.52	63.57
HI7000d	47.71	76.75	100.38	122.36	61.39	106.68	141.10	123.44	204.75	136.35
HI7008a	48.33	249.74	73.86	99.14	65.69	164.45	356.87	142.36	282.89	76.77
Average	70.33	142.91	112.22	117.65	71.09	135.62	194.58	108.18	167.24	84.75

Table 6 Maximum absolute relative error of volume on June 22 and 23, 2011

Segment	Maximum absolute relative error (%)									
	June 22, 2011					June 23, 2011				
	mx_{AK}	mx_{A}	mx_{KF}	mx_{PF}	mx_{EM}	mx_{AK}	mx_{A}	mx_{KF}	mx_{PF}	mx_{EM}
HI2075a	85.96	100.25	142.90	174.90	75.60	222.16	161.20	230.66	220.91	133.09
HI3002b	237.10	416.34	364.61	250.41	203.21	212.46	208.69	178.88	127.25	74.24
HI7000d	80.05	149.08	142.46	157.17	68.73	323.05	1111.94	603.71	187.65	865.45
HI7008a	118.62	371.77	188.25	274.03	130.47	276.37	534.32	264.54	427.29	173.52
Average	130.43	259.36	209.56	214.13	119.50	258.51	504.04	319.45	240.78	311.58

Table 7 Mean relative error sum of squares of speed on June 22 and 23, 2011

Segment	Mean relative error sum of squares (%)									
	June 22, 2011					June 23, 2011				
	rm_{AK}	rm_{A}	rm_{KF}	rm_{PF}	rm_{EM}	rm_{AK}	rm_{A}	rm_{KF}	rm_{PF}	rm_{EM}
HI2075a	0.54	1.08	10.91	12.02	9.27	0.20	2.44	9.51	9.21	7.69
HI3002b	1.25	1.99	17.50	5.90	3.91	0.47	1.54	8.77	3.57	3.90
HI7000d	0.23	0.59	10.06	7.97	6.49	0.27	1.99	10.69	12.78	9.68
HI7008a	0.23	6.24	7.52	9.03	7.76	3.91	12.74	21.64	31.87	7.77
Average	0.56	2.48	11.50	8.73	6.86	1.21	4.68	12.65	14.36	7.26

Table 8 Mean relative error sum of squares of volume on June 22 and 23, 2011

Segment	Mean relative error sum of squares (%)									
	June 22, 2011					June 23, 2011				
	rm_{AK}	rm_{A}	rm_{KF}	rm_{PF}	rm_{EM}	rm_{AK}	rm_{A}	rm_{KF}	rm_{PF}	rm_{EM}
HI2075a	0.74	1.00	14.16	51.53	4.87	2.63	2.60	22.95	40.64	7.67
HI3002b	5.62	17.33	32.97	56.19	11.18	2.13	4.36	17.55	29.43	6.09
HI7000d	0.64	2.22	18.52	30.97	5.01	17.90	124.09	111.07	556.71	207.92
HI7008a	1.41	13.82	26.76	71.68	14.67	3.92	28.55	35.03	118.52	15.59
Average	2.10	8.59	23.10	52.59	8.93	6.65	39.90	46.65	186.33	59.32

Table 9 Mean absolute relative error of speed on June 25 and 26, 2011

Segment	Mean absolute relative error (%)									
	June 25, 2011					June 26, 2011				
	ma_{AK}	ma_{A}	ma_{KF}	ma_{PF}	ma_{EM}	ma_{AK}	ma_{A}	ma_{KF}	ma_{PF}	ma_{EM}
HI2075a	10.35	16.19	26.71	12.15	21.18	7.63	9.69	23.85	10.18	18.91
HI3002b	5.64	8.60	25.94	3.82	11.49	8.11	12.42	23.44	5.88	12.69
HI7000d	7.53	7.92	20.46	7.71	18.87	13.27	13.43	25.70	7.28	6.81
HI7008a	6.74	14.72	23.87	13.15	17.60	12.08	18.53	30.11	16.37	17.78
Average	7.57	11.86	24.25	9.21	17.29	10.25	13.52	25.78	9.93	14.05

Table 10 Mean absolute relative error of volume on June 25 and 26, 2011

Segment	Mean absolute relative error (%)									
	June 25, 2011					June 26, 2011				
	ma_{AK}	ma_{A}	ma_{KF}	ma_{PF}	ma_{EM}	ma_{AK}	ma_{A}	ma_{KF}	ma_{PF}	ma_{EM}
HI2075a	12.94	20.41	12.09	19.38	12.92	11.42	22.37	16.42	22.74	15.13
HI3002b	10.88	20.24	27.13	11.50	14.65	12.42	26.76	27.40	14.09	16.63
HI7000d	11.58	21.03	27.91	11.67	13.65	15.52	18.35	35.17	16.62	15.41
HI7008a	17.30	40.35	32.47	16.26	14.06	23.31	34.68	39.39	30.16	25.90
Average	13.18	25.51	24.90	14.70	13.82	15.67	25.54	29.60	20.90	18.27

Table 11 Maximum absolute relative error of speed on June 25 and 26, 2011

Segment	Maximum absolute relative error (%)									
	June 25, 2011					June 26, 2011				
	mx_{AK}	mx_{A}	mx_{KF}	mx_{PF}	mx_{EM}	mx_{AK}	mx_{A}	mx_{KF}	mx_{PF}	mx_{EM}
HI2075a	59.24	118.19	108.88	92.51	68.57	35.86	55.33	84.47	128.07	73.86
HI3002b	49.18	74.01	66.18	18.88	23.57	52.42	148.09	102.52	73.17	44.49
HI7000d	36.82	41.46	53.14	35.10	50.86	54.96	126.42	85.99	54.52	50.57
HI7008a	46.21	109.40	51.44	84.41	68.68	68.68	103.27	185.83	210.58	146.58
Average	47.86	85.77	69.91	57.73	52.92	52.98	108.28	114.70	116.59	78.88

Table 12 Maximum absolute relative error of volume on June 25 and 26, 2011

Segment	Maximum absolute relative error (%)									
	June 25, 2011					June 26, 2011				
	mx_{AK}	mx_{A}	mx_{KF}	mx_{PF}	mx_{EM}	mx_{AK}	mx_{A}	mx_{KF}	mx_{PF}	mx_{EM}
HI2075a	66.40	108.89	73.08	118.45	54.25	63.30	138.31	140.75	183.59	50.86
HI3002b	50.62	90.30	92.85	59.54	63.92	61.25	166.87	104.06	86.23	63.64
HI7000d	95.36	139.28	144.27	103.43	76.09	89.98	72.20	134.19	100.15	58.68
HI7008a	94.15	265.61	126.62	81.03	52.03	337.14	262.68	316.12	490.36	242.86
Average	76.63	151.02	109.21	90.61	61.57	137.92	160.02	173.78	215.08	104.01

Table 13 Mean relative error sum of squares of speed on June 25 and 26, 2011

Segment	Mean relative error sum of squares (%)									
	June 25, 2011					June 26, 2011				
	rm_{AK}	rm_{A}	rm_{KF}	rm_{PF}	rm_{EM}	rm_{AK}	rm_{A}	rm_{KF}	rm_{PF}	rm_{EM}
HI2075a	2.40	7.64	10.37	5.10	6.11	1.24	2.05	7.39	5.71	4.94
HI3002b	0.87	2.05	8.13	0.27	1.52	1.63	6.29	7.95	1.25	2.27
HI7000d	1.14	1.24	5.58	1.21	4.63	3.09	5.26	8.80	1.52	1.13
HI7008a	1.16	6.02	7.02	5.09	4.78	3.48	7.93	15.18	11.34	6.59
Average	1.39	4.24	7.78	2.92	4.26	2.36	5.38	9.83	4.96	3.73

Table 14 Mean relative error sum of volume on June 25 and 26, 2011

Segment	Mean relative error sum of squares (%)									
	June 25, 2011					June 26, 2011				
	rm_{AK}	rm_{A}	rm_{KF}	rm_{PF}	rm_{EM}	rm_{AK}	rm_{A}	rm_{KF}	rm_{PF}	rm_{EM}
HI2075a	3.69	9.64	9.64	8.23	3.25	2.56	10.57	7.73	12.95	3.60
HI3002b	2.56	7.68	7.68	2.69	3.90	3.58	17.38	12.22	4.61	4.60
HI7000d	3.04	10.13	10.13	3.07	3.09	5.18	5.85	18.84	6.39	4.60
HI7008a	6.31	35.88	35.88	4.99	3.56	26.16	33.97	43.54	53.46	20.09
Average	3.90	15.83	15.83	4.75	3.45	9.37	16.94	20.58	19.35	8.22

Table 15 Speed and volume statistical significance

Date	Statistical significance							
	Speed				Volume			
	HI2075a	HI3002b	HI7000d	HI7008a	HI2075a	HI3002b	HI7000d	HI7008a
June 22, 2011	−1.36	−2.33	−3.26	−2.05	−3.26	−4.15	−3.41	−2.21
June 23, 2011	−8.53	−8.55	−8.81	−8.67	−8.81	−8.82	−9.05	−8.80
June 25, 2011	−2.33	−2.03	−3.18	−2.30	−3.08	−3.42	−1.95	−1.63
June 26, 2011	−0.93	−1.33	−2.26	−2.81	−3.29	−3.18	−1.66	−2.57

5 Conclusions

Three conclusions can be drawn by comparing the real-time prediction analysis results of the ARIMA–Kalman model with those from the pure ARIMA model, the Kalman filter, particle filter, and expectation maximization algorithm:

1. The mean absolute relative prediction error of speed data based on the proposed algorithm is lower than those of the pure ARIMA model, the Kalman filter, and the particle filter mentioned above, indicating that the proposed algorithm has a higher accuracy.

2. According to the maximum absolute relative error of the prediction, traffic state prediction based on the ARIMA–Kalman model performs admirably in tracking trends in the variation of the traffic state. The mean relative error sum of squares signifies that the proposed algorithm is more stable than the pure ARIMA model and Kalman filter.

3. The proposed algorithm is easy to implement on a computer, and is suitable for online prediction of the road traffic state, because it has fewer variable types and dynamic cumulative values compared with pure ARIMA–Kalman methods.

Considering the remarkable performance of the proposed algorithm, we will explore traffic state prediction based on spatial–temporal correlations in our next study.

References

Brockwell, P.J., Davis, R.A., 2006. ARMA models. *In*: Casella, G., Fienberg, S., Olkin, I. (Eds.), Introduction to Time Series and Forecasting. Springer Science & Business Media, Berlin, Germany, p.83-100.

Chang, T.H., Chueh, C.H., Yang, L.K., 2011. Dynamic traffic prediction for insufficient data roadways via automatic control theories. *Contr. Eng. Pract.*, **19**(12):1479-1489. http://dx.doi.org/10.1016/j.conengprac.2011.08.007

Chen, B.K., Xie, Y.B., Tong, W., *et al*., 2012. A comprehensive study of advanced information feedbacks in real-time intelligent traffic systems. *Phys. A*, **91**(8):2730-2739. http://dx.doi.org/10.1016/j.physa.2011.12.032

Chen, C.Y., Hu, J.M., Meng, Q., *et al*., 2011. Short-time traffic flow prediction with ARIMA-GARCH model. IEEE

Intelligent Vehicles Symp., p.607-612. http://dx.doi.org/10.1109/IVS.2011.5940418

Diebold, F.X., Mariano, R.S., 1995. Comparing predictive accuracy. *J. Bus. Econ. Stat.*, **13**(3):134-144. http://dx.doi.org/10.1198/073500102753410444

Dong, C.F., Ma, X., Wang, G.W., *et al*., 2009. Prediction feedback in intelligent traffic systems. *Phys.*, **388**(21): 4651-4657. http://dx.doi.org/10.1016/j.physa.2009.07.018

Dong, C.F., Ma, X., Wang, B.H., 2010. Weighted congestion coefficient feedback in intelligent transportation systems. *Phys. Lett. A*, **374**(11):1326-1331. http://dx.doi.org/10.1016/j.physleta.2010.01.011

Durbin, J., Koopman, S.J., 2012. Time Series Analysis by State Space Methods. Oxford University Press, London, UK.

Guo, J.H., Huang, W., Williams, B.M., 2014. Adaptive Kalman filter approach for stochastic short-term traffic flow rate prediction and uncertainty quantification. *Transp. Res. Part C*, **43**:50-64. http://dx.doi.org/10.1016/j.trc.2014.02.006

Hoong, P.K., Tan, I.K.T., Chien, O.K., *et al*., 2012. Road traffic prediction using Bayesian networks. IET Int. Conf. on Wireless Communications and Applications, p.1-5. http://dx.doi.org/10.1049/cp.2012.2098

Kirchgässner, G., Wolters, J., Hassler, U., 2012. Introduction to Modern Time Series Analysis. Springer Science & Business Media, Berlin, Germany.

Kumar, K., Parida, M., Katiyar, V.K., 2013. Short term traffic flow prediction for a non urban highway using artificial neural network. *Proc.-Soc. Behav. Sci.*, **104**:755-764. http://dx.doi.org/10.1016/j.sbspro.2013.11.170

Lin, L., Li, Y., Sadek, A., 2013. A *k* nearest neighbor based local linear wavelet neural network model for online short-term traffic volume prediction. *Proc.-Soc. Behav. Sci.*, **96**:2066-2077. http://dx.doi.org/10.1016/j.sbspro.2013.08.223

Liu, H., Tian, H.Q., Li, Y.F., 2012. Comparison of two new ARIMA-ANN and ARIMA-Kalman hybrid methods for wind speed prediction. *Appl. Energy*, **98**:415-424. http://dx.doi.org/10.1016/j.apenergy.2012.04.001

Liu, J.Y., Wang, W.D., Gong, X.Y., *et al*., 2012. A hybrid model based on Kalman filter and neutral network for traffic prediction. IEEE 2nd Int. Conf. on Cloud Computing and Intelligent Systems, p.533-536. http://dx.doi.org/10.1109/CCIS.2012.6664231

Liu, X.L., Jia, P., Wu, S.H., *et al*., 2011. Short-term traffic flow forecasting based on multi-dimensional parameters. *J. Transp. Syst. Eng. Inform. Technol.*, **11**(4):140-146 (in Chinese).

Lv, L., Chen, M., Liu, Y., *et al*., 2015. A plane moving average algorithm for short-term traffic flow prediction. *In*: Cau, T., Lim, E.P., Zhou, Z.H., *et al.* (Eds.), Advances in Knowledge Discovery and Data Mining. Springer Int. Publishing, Cham, Switzerland, p.357-369. http://dx.doi.org/10.1007/978-3-319-18032-8_28

Ma, T., Zhou, Z., Abdulhai, B., 2015. Nonlinear multivariate time–space threshold vector error correction model for short term traffic state prediction. *Transp. Res. Part B*, **76**:27-47. http://dx.doi.org/10.1016/j.trb.2015.02.008

Ma, X.L., Tao, Z.M., Wang, Y.H., *et al*., 2015. Long short-term memory neural network for traffic speed prediction using remote microwave sensor data. *Transp. Res. Part C*, **54**:187-197. http://dx.doi.org/10.1016/j.trc.2015.03.014

Min, W., Wynter, L., 2011. Real-time road traffic prediction with spatio-temporal correlations. *Transp. Res. Part C*, **19**(4):606-616. http://dx.doi.org/10.1016/j.trc.2010.10.002

Moretti, F., Pizzuti, S., Panzieri, S., *et al*., 2015. Urban traffic flow forecasting through statistical and neural network bagging ensemble hybrid modeling. *Neurocomputing*, **167**:3-7. http://dx.doi.org/10.1016/j.neucom.2014.08.100

Ojeda, L.L., Kibangou, A.Y., de Wit, C.C., 2013. Adaptive Kalman filtering for multi-step ahead traffic flow prediction. IEEE American Control Conf., p.4724-4729. http://dx.doi.org/10.1109/ACC.2013.6580568

Pan, T.L., Sumalee, A., Zhong, R.X., *et al*., 2013. Short-term traffic state prediction based on temporal–spatial correlation. *IEEE Trans. Intell. Transp. Syst.*, **14**(3):1242-1254. http://dx.doi.org/10.1109/TITS.2013.2258916

Park, J., Li, D., Murphey, Y.L., *et al*., 2011. Real time vehicle speed prediction using a neural network traffic model. IEEE Int. Joint Conf. on. Neural Networks, p.2991-2996. http://dx.doi.org/10.1109/IJCNN.2011.6033614

Qi, Y., Ishak, S., 2014. A hidden Markov model for short term prediction of traffic conditions on freeways. *Transp. Res. Part C*, **43**:95-111. http://dx.doi.org/10.1016/j.trc.2014.02.007

Smith, B.L., Williams, B.M., Oswald, R.K., 2002. Comparison of parametric and nonparametric models for traffic flow forecasting. *Transp. Res. Part C*, **10**(4):303-321. http://dx.doi.org/10.1016/S0968-090X(02)00009-8

Sommer, M., Tomforde, S., Haehner, J., 2015. A systematic study on forecasting of traffic flows with artificial neural networks. Proc. 28th Int. Conf. on. Architecture of Computing Systems, p.1-8.

Vlahogianni, E.I., Karlaftis, M.G., Golias, J.C., 2005. Optimized and meta-optimized neural networks for short-term traffic flow prediction: a genetic approach. *Transp. Res. Part C*, **13**(3):211-234. http://dx.doi.org/10.1016/j.trc.2005.04.007

Wang, J., Shi, Q.X., 2013. Short-term traffic speed forecasting hybrid model based on chaos–wavelet analysis-support vector machine theory. *Transp. Res. Part C*, **27**:219-232. http://dx.doi.org/10.1016/j.trc.2012.08.004

Zhang, L., Ma, J., Sun, J., 2012. Examples of validating an adaptive Kalman filter model for short-term traffic flow prediction. 12th Int. Conf. of Transportation Professionals, p.912-922. http://dx.doi.org/10.1061/9780784412442.094

Zhang, L., Liu, Q.C., Yang, W.C., *et al*., 2013. An improved *k*-nearest neighbor model for short-term traffic flow prediction. *Proc.-Soc. Behav. Sci.*, **96**:653-662. http://dx.doi.org/10.1016/j.sbspro.2013.08.076